

Phosphorylation-regulated axonal dependent transport of syntaxin 1 is mediated by a Kinesin-1 adapter

John Jia En Chua^a, Eugenia Butkevich^b, Josephine M. Wörseck^c, Maike Kittelmann^d, Mads Grønberg^a, Elmar Behrmann^a, Ulrich Stelzl^f, Nathan J. Pavlos^a, Maciej M. Lalowski^{e,1}, Stefan Eimer^d, Erich E. Wanker^e, Dieter Robert Klopfeinstein^{b,f,2}, and Reinhard Jahn^{a,2}

^aDepartment of Neurobiology, Max-Planck-Institute for Biophysical Chemistry, 37077 Göttingen, Germany; ^bGeorg-August-Universität Göttingen, Drittes Physikalisches Institut-Biophysik, 37077 Göttingen, Germany; ^cBiochemistry II, Georg-August-Universität Göttingen, 37073 Göttingen, Germany; ^dMax-Planck-Institute for Molecular Genetics, 14195 Berlin, Germany; ^eEuropean Neuroscience Institute Göttingen and German Research Foundation Research Center for Molecular Physiology of the Brain, 37077 Göttingen, Germany; and ^fMax Delbrück Center for Molecular Medicine, 13092 Berlin-Buch, Germany

Edited by Ronald D. Vale, University of California, San Francisco, CA, and approved March 5, 2012 (received for review August 22, 2011)

Presynaptic nerve terminals are formed from preassembled vesicles that are delivered to the prospective synapse by kinesin-mediated axonal transport. However, precisely how the various cargoes are linked to the motor proteins remains unclear. Here, we report a transport complex linking syntaxin 1a (Stx) and Munc18, two proteins functioning in synaptic vesicle exocytosis at the presynaptic plasma membrane, to the motor protein Kinesin-1 via the kinesin adaptor FEZ1. Mutation of the FEZ1 ortholog UNC-76 in *Caenorhabditis elegans* causes defects in the axonal transport of Stx. We also show that binding of FEZ1 to Kinesin-1 and Munc18 is regulated by phosphorylation, with a conserved site (serine 58) being essential for binding. When expressed in *C. elegans*, wild-type but not phosphorylation-deficient FEZ1 (S58A) restored axonal transport of Stx. We conclude that FEZ1 operates as a kinesin adaptor for the transport of Stx, with cargo loading and unloading being regulated by protein kinases.

fasciculation and elongation protein zeta 1 | transport defect | cargo aggregation

The formation and maintenance of presynaptic boutons are intricate but highly efficient processes during which the machinery for exocytosis and recycling of synaptic vesicles is assembled from preformed units. These units are delivered to the nascent synapse via molecular motor proteins of the kinesin superfamily (reviewed in Ref. 1).

Although Kinesin-3 appears to be the main motor transporting synaptic vesicle precursors, recent evidence suggests that Kinesin-1 (KIF5) is also involved. In *Drosophila*, deletion of UNC-76/fasciculation and elongation protein zeta 1 (FEZ1), a specific adaptor for Kinesin-1, left synaptic vesicles stranded in the axon (2, 3), showing that Kinesin-1 is needed at least during later phases of axonal transport. Transport of the synaptic vesicle protein synaptotagmin by the UNC-76/Kinesin-1 complex requires phosphorylation of UNC-76 by the UNC-51/ATG1 kinase, a prerequisite for UNC-76 to bind synaptotagmin (3). Deletion of this kinase phenocopies deletion of UNC-76. Indeed, phosphorylation-regulated interactions between cargo, adaptors, and kinesins have also been observed for other transport complexes such as the kinesin light chain/JIP1 (c-Jun N-terminal kinase-interacting protein 1) complex (4). This suggests that phosphorylation is a common mechanism for the regulation of kinesin-based transport complexes (5).

Less is known about the involvement of Kinesin-1 in the transport of other classes of synaptic precursor vesicles. Transport of syntaxin 1a (Stx), an essential component of the exocytotic release apparatus residing in the presynaptic plasma membrane, is clearly distinct from synaptic vesicle precursors and appears to involve a complex between Kinesin-1 and the Stx-binding protein syntabulin (6, 7). Down-regulation or expression of dominant-negative syntabulin reduces but does not abolish membrane delivery of Stx, indicating the existence of other transport mechanisms (6). Moreover, proper intracellular trafficking of Stx and its function in exocytosis depends on Munc18 coexpression (8–14). Stx trafficking defects were observed in *unc-18* knockouts in *Caenorhabditis elegans* (14), Munc18 knockdowns in PC12 cells (9, 13) but not in mouse Munc18-1

knockouts (15), although in the latter case, a compensation by other Munc18 isoforms cannot be excluded. These defects were attributed to a need for Stx to be stabilized by Munc18 in the inactive conformation during transport to prevent it from being trapped in nonproductive SNARE complexes (10) but Munc18 could additionally participate in loading Stx onto kinesin. Here, we identify and characterize a putative transport complex including Stx, Munc18, FEZ1, and the Kinesin-1 family member KIF5C.

Results

FEZ1 Interacts with Stx and Munc18. We recently initiated an effort to systematically identify interaction partners of established presynaptic proteins using an automated yeast two-hybrid (Y2H) screen. Bait proteins corresponding to defined regions of these proteins were tested against an arrayed matrix containing human full-length ORF prey constructs. As part of the data stemming from this screen, we discovered that the Kinesin-1 adaptor FEZ1 binds both to Stx and Munc18 (Fig. 1A). These results suggested an alternative, Munc18-dependent, transport route for plasma membrane delivery of Stx in addition to the reported syntabulin-dependent pathway.

To validate the interactions, lysates of HEK 293 cells transiently expressing GFP-FEZ1 and Myc-Stx, or FLAG-Munc18 constructs were immunoprecipitated with a GFP antibody and analyzed by immunoblotting. FEZ1 readily precipitated both Stx (Fig. 1B) and Munc18 (Fig. 1C). FEZ1 also precipitated Munc18 in reciprocal coimmunoprecipitations (Fig. S1). These results validate the Y2H identified interactions and show that FEZ1 specifically interacts with both Munc18 and Stx in mammalian cells.

The Y2H screening revealed that the N terminus of FEZ1 mediates interaction with neither presynaptic protein as a FEZ1 prey containing amino acids 8–91 tested did not yield viable colonies (Fig. 1A). Additionally, FEZ1 binds amino acids 246–449 of Munc18. To determine which FEZ1 region binds Stx and Munc18, GFP-FEZ1 deletion mutants (Fig. S2A) were tested in coimmunoprecipitations as described above. Munc18 coprecipitated with both full-length FEZ1 and its N-terminal fragment (amino acids 1–310) (Fig. S2B). A further deletion of amino acids 221–310 of FEZ1 abolished Munc18 binding, indicating that the region is primarily responsible for this interaction. The region contains a coiled-coil domain reported to bind other proteins and is evolutionarily conserved (16). An even shorter

Author contributions: J.J.E.C., S.E., E.E.W., D.R.K., and R.J. designed research; J.J.E.C., E. Butkevich, J.M.W., M.K., M.G., and E. Behrmann performed research; M.M.L. contributed new reagents/analytic tools; J.J.E.C., E. Butkevich, J.M.W., M.K., M.G., U.S., N.J.P., and D.R.K. analyzed data; and J.J.E.C. and R.J. wrote the paper.

The authors declare no conflict of interest.

This article is a PNAS Direct Submission.

¹Present address: Protein Chemistry/Proteomics/Peptide Synthesis and Array Unit, Biomedicum Helsinki, University of Helsinki, FI-00014 Helsinki, Finland.

²To whom correspondence may be addressed. E-mail: dklopfe@gwdg.de or rjahn@gwdg.de.

This article contains supporting information online at www.pnas.org/lookup/suppl/doi:10.1073/pnas.1113819109/-DCSupplemental.

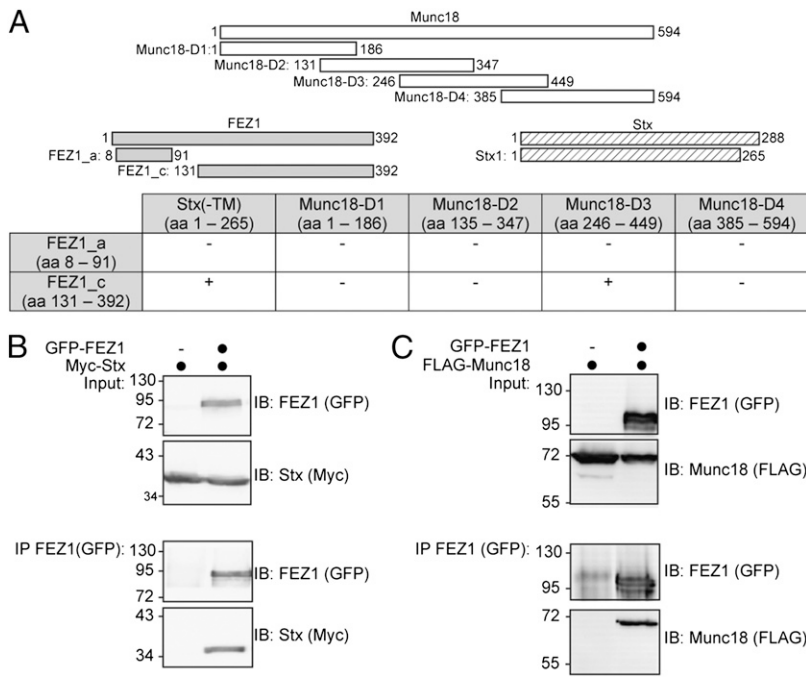


Fig. 1. FEZ1 interacts with Munc18 and Stx. (A) Identification of FEZ1 as an interactor of Munc18 and Stx using a Y2H assay. Bait constructs containing fragments of Munc18 and Stx (without its transmembrane domain) were used to screen preys containing different FEZ1 fragments [amino acid residues (aa) given in parentheses]. (B and C) Validation of FEZ1 interactions by coimmunoprecipitation. HEK 293 cells expressing tagged FEZ1 with either Stx or Munc18 (black circles on top of the lanes) were immunoprecipitated (IP) using tag-specific antibodies (anti-GFP) and analyzed by immunoblotting (IB) for the presence of GFP-FEZ1, Myc-Stx, and FLAG-Munc18, respectively. FEZ1 interacts with both Munc18 and Stx. Input corresponds to 1% of the starting material used for immunoprecipitation. Molecular mass markers indicated are in kilodaltons.

FEZ1 peptide (amino acids 131–210) also did not bind Munc18. Additional mapping of the Munc18 binding domain of FEZ1 with peptides containing only its coiled-coil domain or additional flanking segments (Fig. S2A) confirmed that the coiled-coil domain suffices to bind Munc18 (Fig. S2B). However, the interaction is considerably weaker compared with the N-terminal fragment (amino acids 1–310). Because the N-terminal domain of FEZ1 mediates its dimerization (17), we speculate that FEZ1 dimerization enhances its binding to Munc18.

Likewise, binding of Stx to FEZ1 progressively decreased when the coiled-coil domain was removed (Fig. S2C; compare amino acids 1–310 with amino acids 1–220). Only background binding was observed when amino acids 131–210 of FEZ1 were used to coimmunoprecipitate Stx (see also Fig. 2).

FEZ1 Forms a Transport Complex with Stx, Munc18, and Kinesin-1.

The Sec1/Munc18 protein binds to Stx (12). Thus, the three proteins may form a tripartite complex in vivo. Indeed, immunoprecipitation of FEZ1 in HEK 293 cells expressing all three proteins efficiently pulls down both Munc18 and Stx (Fig. 2A). Deletion of the coiled-coil domain of FEZ1 responsible for binding to Munc18 does not abolish formation of this complex, suggesting that, at least under these conditions, binding of Munc18 to FEZ1 is indirect, being mediated by binding to Stx. This finding also excludes the possibility that coprecipitation of both Munc18 and Stx is attributable to the isolation of two distinct FEZ1 binary complexes (i.e., FEZ1-Munc18 versus FEZ1-Stx complexes).

FEZ1 binds Kinesin-1 and is involved in synaptic vesicle transport (2, 3, 18). We wondered whether FEZ1 might also

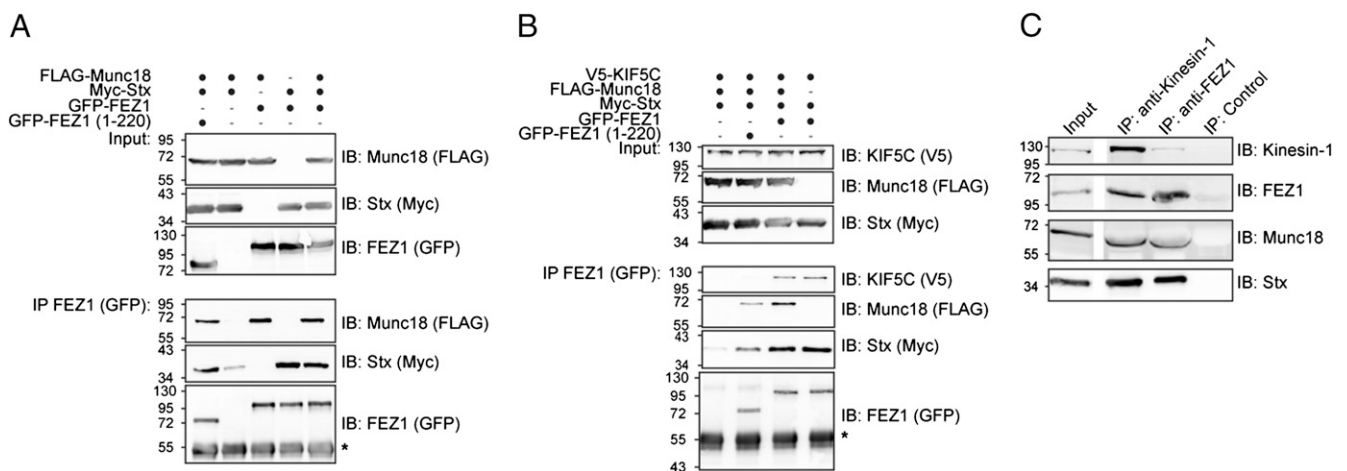


Fig. 2. Protein complexes formed by FEZ1 reveal its function as cargo adaptor for Kinesin-1 (KIF5C). (A and B) HEK 293 cells expressing combinations of tagged versions of FEZ1, Munc18, KIF5C, or Stx were immunoprecipitated (IP) using anti-GFP antibodies and immunoblotted (IB) using tag-specific antibodies (anti-FLAG, anti-GFP, anti-Myc, or anti-V5). Molecular mass markers are indicated are in kilodaltons. *Ig heavy chain. (A) FEZ1 forms a trimeric complex with Munc18 and Stx. Full-length and FEZ1 (amino acids 1–220) efficiently immunoprecipitate Stx and Munc18 indicating that direct binding of Munc18 to FEZ1 is not necessary for trimeric complex formation. (B) KIF5C, FEZ1, Stx, and Munc18 can be concurrently isolated as a complex. In addition, binding of Stx to KIF5C can occur without Munc18 but is dependent on the presence of the coiled-coil domain of FEZ1. (C) The FEZ1/Kinesin-1 transport complex comprising FEZ1, Stx, Munc18, and Kinesin-1 can be immunisolated from rat brain postnuclear supernatants using anti-FEZ1 or anti-Kinesin-1 antibodies.

similarly transport Stx and/or Munc18. We first investigated how these proteins interact with Kinesin-1. Binding of Stx to Kinesin-1 is dependent on syntabulin, another motor adaptor protein (6). Immunoprecipitation of Munc18 from cell lysates after cotransfection of Munc18 with Kinesin-1 (KIF5C) revealed both proteins do not directly interact (Fig. S3A). As reported, FEZ1 coprecipitates with Kinesin-1 (KIF5C) (Fig. S3B, lane 1) (18). In triple transfections with FEZ1, KIF5C, and either Munc18 or Stx, immunoprecipitation of FEZ1 resulted in efficient coprecipitation of either set of proteins, demonstrating that FEZ1 indeed functions as a kinesin adaptor for Munc18 and Stx (Fig. 2B, right lane, and Fig. S3B).

Importantly, immunoprecipitation of FEZ1 in quadruple-transfected cells with all four proteins resulted in the isolation of the Munc18-Stx-FEZ1-KIF5C quaternary complex (Fig. 2B, lane 3). As a further control, we replaced full-length FEZ1 with the truncated version (amino acids 1–220) that is unable to bind Kinesin-1 and Munc18. Here, FEZ1 (amino acids 1–220), Stx, and Munc18 can still be concomitantly isolated, but, as expected, KIF5C does not coprecipitate (Fig. 2B, lane 2).

To confirm that FEZ1 actually binds Kinesin-1 to Stx and Munc18 in neurons, we prepared postnuclear supernatants from the rat brain and then immunoprecipitated FEZ1-containing cargo-motor complexes using anti-FEZ1 antibody-coupled magnetic microbeads. Kinesin-1, Munc18, and Stx were readily detected in immunoprecipitated FEZ1 complexes (Fig. 2C). Reciprocal coimmunoprecipitation using anti-Kinesin-1 antibody also coprecipitated FEZ1, Munc18, and Stx. In summary, the experiments here support the existence of a FEZ1/Kinesin-1 transport complex containing Stx and Munc18 in vivo, with FEZ1 serving as a central scaffold to connect cargo and motor using overlapping yet distinct binding domains.

Mutation of UNC-76 in *C. elegans* Impairs Axonal Transport of Stx.

During axonal outgrowth, Stx is not transported together with synaptic vesicle precursors (19, 20) but in separate vesicles that have not been characterized to date. Our results indicate that FEZ1 may serve as a Kinesin-1 motor adaptor for Stx and Munc18. In view of the role of FEZ1 in neuritogenesis and microtubule-based transport (21), we hypothesized that FEZ1-dependent transport of both proteins may already function during early axonogenesis. Indeed, FEZ1 is present and localizes well with α -tubulin in neuronal growth cones of young neurons (Fig. 3A). As previously reported, Stx and Munc18 are also present in growth cones (22, 23), where they extensively colocalize as expected from their tight association (Fig. 3B and C). Importantly, both proteins also strongly colocalize with FEZ1, indicating they are likely to be transported by FEZ1 in young neurons (Fig. 3D–F).

Although the data indicate these proteins association in neurons, the approach is unable to determine whether FEZ1/Kinesin-1 is responsible for their transport in vivo. We, therefore, tested whether the distributions of Stx and Munc18 in axons are affected if FEZ1 is absent. Because all proteins under investigation are highly conserved evolutionarily, these experiments were conducted in *C. elegans*, an organism that has been extensively used to study axonal transport (24). Mutations in each of the four proteins are known to result in an uncoordinated phenotype typical for most defects in synaptic transmission (25–29), with the orthologs being UNC-18 (Munc18), UNC-76 (FEZ1), UNC-64 (Stx), and UNC-116 (Kinesin-1).

Coimmunoprecipitation of tagged *C. elegans* variants expressed from HEK 293 cells confirmed that interactions between FEZ1, Stx and Munc18 are conserved in worms (Fig. S5). In transgenic worm strains expressing GFP-UNC-64 or GFP-UNC-18, both proteins show diffuse cytoplasmic distribution in processes of ventral nerve cord (VNC) neurons (Fig. 4A, a and f). If UNC-76 is involved in anterograde trafficking of either protein, lack of UNC-76 should leave them stranded in the cell body and/or the axons. Indeed, in *unc-76* mutants, the distribution of GFP-UNC-64 was more irregular than in wild-type controls, with clusters becoming clearly visible in axons and sometimes also observable within cell bodies (Fig. 4A, a vs. b; also Fig. S6A). Quantification by quantitative image analyses confirmed significantly greater

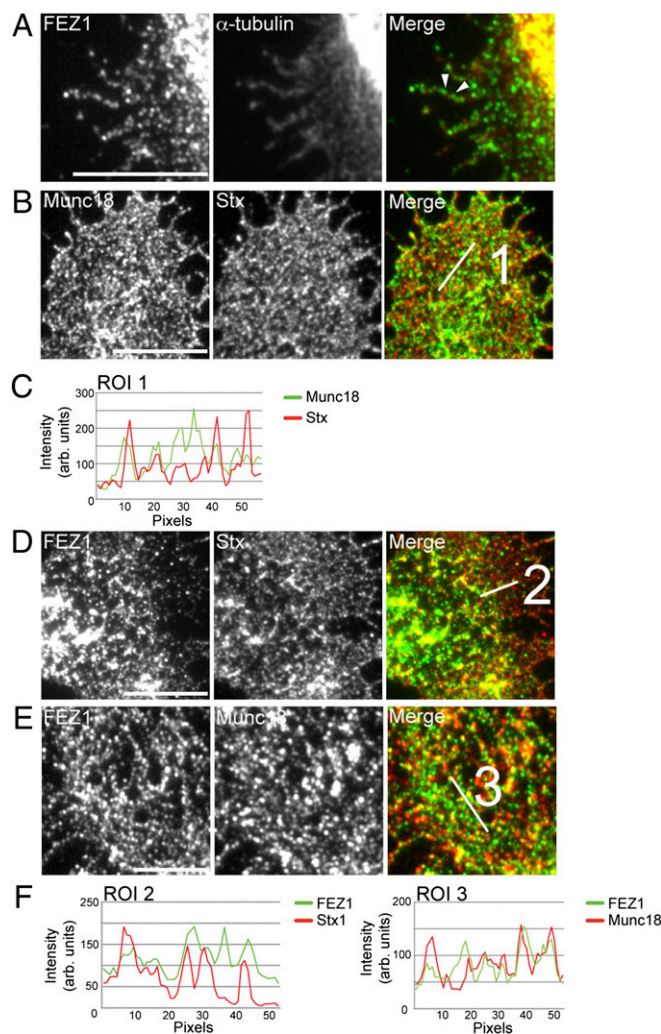


Fig. 3. FEZ1 colocalizes with Stx, Munc18, and α -tubulin in neuronal growth cones. Two to three DIV neurons were fixed and stained for endogenous FEZ1, Stx, Munc18, or α -tubulin. (A) Numerous FEZ1 puncta are observed in neuronal growth cones that are strongly microtubule-associated (e.g., arrowheads). (B) Stx and Munc18 colocalizes in growth cones as expected. FEZ1 colocalizes with Stx (D) and Munc18 (E) in growth cones. Line scans of regions of interest indicated are shown in C and F. (Scale bars, 10 μ m.) Correlation coefficients for each colocalization pair are 0.88 ± 0.02 (Munc18+Stx), 0.802 ± 0.02 (FEZ1+Stx), and 0.75 ± 0.02 (FEZ1+Munc18), respectively. Eight growth cones were taken for each set of analysis. Images of the entire growth cones are shown in Fig. S4.

clustering of GFP-UNC-64 in ventral cord neurons of *unc-76* mutant animals (Fig. 4B). This phenotype is similar in appearance to axonal aggregates of synaptic vesicles seen in *Drosophila* lacking FEZ1 or Kinesin-1, which was attributed to defects in axonal transport following loss of either protein (2, 3). Importantly, GFP-UNC-64 distribution anomalies were completely rescued by pan-neuronal expression of wild-type UNC-76 in these mutants (Fig. 4A, d, and 4B). This result demonstrates that loss of UNC-76/FEZ1 in neurons specifically cause formation of GFP-UNC-64 aggregates. In contrast, no major changes were seen in the distribution of GFP-UNC-18 in neither *unc-76* nor *unc-116* mutants (Fig. 4A, f–h, and 4B; also Fig. S6B). Nevertheless, it is plausible that the soluble pool of UNC-18 occludes changes of UNC-18 associated with the Stx transport vesicles.

Deletion of UNC-116 also phenocopied the transport defect of Stx-containing vesicles in *unc-76* mutants (Fig. 4A, c, and Fig. S6A). Quantification of clustering indicates that *unc-116* mutants exhibited an even more pronounced phenotype (Fig. 4B)

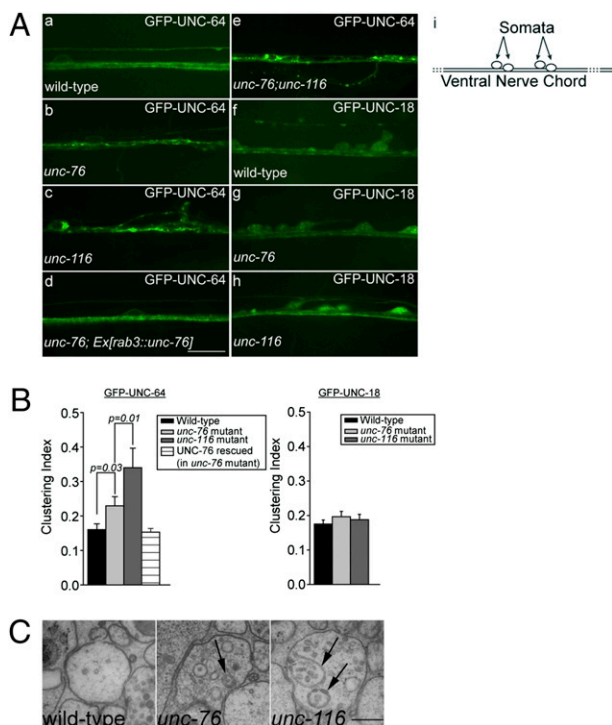


Fig. 4. Mutation of FEZ1 (*unc-76*) affects trafficking of syntaxin (UNC-64) in ventral nerve cords of *C. elegans*. (A) Axonal distribution of GFP-tagged UNC-64 and UNC-116 in wild-type and mutant *C. elegans*. (a–c) Distribution of GFP-UNC-64 differs between wild-type (a), *unc-76* (*e911*) mutants (b), and *unc-116* (*e2310*) mutants (c). (c) *Unc-116* mutants exhibit greater axonal clustering of GFP-UNC-64 than *unc-76* mutants (b). Expression of mCherry-UNC-76 rescues GFP-UNC-64 clustering in *unc-76* mutants (d). *Unc-76;unc-116* double mutants exhibit both axonal clustering and significantly more GFP-UNC-64 accumulation in cell bodies (e). Expression patterns of GFP-UNC-18 in wild-type (f), *unc-76* (g), and *unc-116* (h) mutants show no significant differences. (Scale bar, 10 μ m.) Diagram in *i* shows the schematic organization of *C. elegans* ventral nerve chord (VNC) as a continuous row of neuronal cell bodies (somata) with axonal bundles running adjacent to the ventral hypodermis. En passant synapses between motor neurons and muscle arms are regularly spaced along the entire length of the VNC. (B) Quantification of GFP-UNC-64 and GFP-UNC-18 clustering using intensity variations along the nerve (line scan analyses). SDs of pixel intensities obtained from the line scans were used to compute an index to compare the extent of clustering (SI Text). Eight to nine worms were taken for each analysis. Error bars represent SEM. (C) Abnormal membranous structures and autophagosomes (arrows) were found within neurites of the ventral cord neurons in *unc-116* and *unc-76* mutants but not in wild-type animals. (Scale bar, 200 nm.)

compared to *unc-76* mutants, as would be expected if the motor function itself was directly disrupted. Importantly, *unc-76;unc-116* double mutants exhibit the strongest transport defect with significant amounts of GFP-UNC-64 being retained as large accumulations in cell bodies in addition to the aforementioned axonal aggregates (Fig. 4A, e). Indeed, the percentage of such cells is highest in double mutants (47.06%, $n = 119$) compared with *unc-116* (33.93%, $n = 56$) or *unc-76* (16.51%, $n = 109$) mutants or wild-type background (3.70%, $n = 108$).

Finally, using electron microscopy, we indeed observed accumulation of abnormal membranous structures in axonal processes of ventral cord neurons in both *unc* mutants (Fig. 4C). Whereas wild-type axons are normally devoid of vesicular clusters, *unc-76* and *unc-116* mutant axons contain clusters of vesicular structures including synaptic and dense core vesicles, multivesicular bodies, and autophagosomes (Fig. 4C). These clusters are more pronounced in *unc-116* mutants compared with *unc-76* mutants. The appearance of autophagosomes surrounding aberrant vesicle clusters in the mutants might represent an attempt to clear these aggregates from the axons.

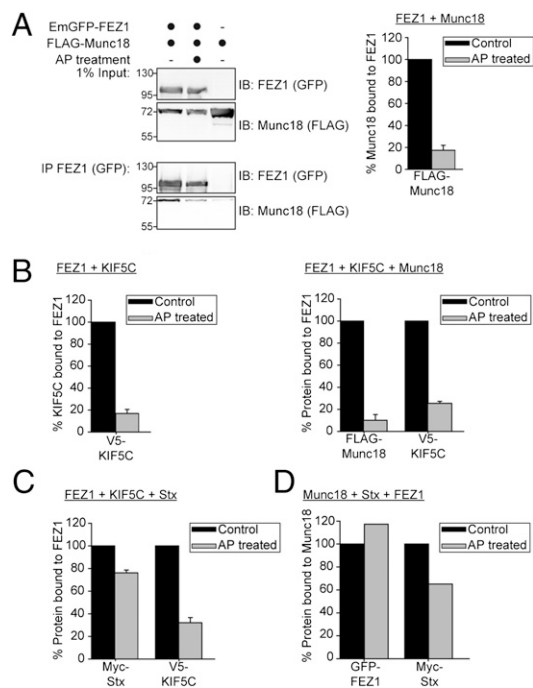


Fig. 5. Phosphorylation of FEZ1 regulates binding to its interaction partners. HEK 293 cell lysates expressing combinations of tagged versions of FEZ1, Munc18, KIF5C, or Stx treated with or without AP were immunoprecipitated using tag-specific antibody (anti-GFP) and immunoblotted using tag-specific antibodies (anti-FLAG, anti-GFP, anti-Myc, or anti-V5). The amount of immunoprecipitated protein was determined by densitometry, with the untreated sample serving as reference (100%). A representative Western blot is shown in A. Data in A–C were obtained from three independent experiments. Error bars represent SDs. (A) Treatment of cell lysates with AP significantly reduces Munc18 binding to FEZ1. (B) Phosphorylation regulates assembly of the trimeric FEZ1-Munc18-Kinesin-1 complex. Dephosphorylation of FEZ1 reduced its binding to KIF5C (left chart) and dissociates the ternary complex of FEZ1, Munc18, and KIF5C (right chart). (C) Dephosphorylation reduces the amount of KIF5C bound to FEZ1 but significant amounts of Stx remain bound to FEZ1. (D) Significant amounts of FEZ1-Stx-Munc18 complexes remain isolatable even after AP treatment. HEK 293 cell lysates expressing tagged versions of Munc18, Stx, and FEZ1 treated with or without AP were immunoprecipitated with tag-specific (anti-FLAG) antibody and immunoblotted using tag-specific antibodies (anti-FLAG, anti-Myc, or anti-GFP). Data were obtained from the average of two independent experiments.

Together, these results demonstrate that UNC-76 functions as an adaptor that links UNC-64 to UNC-116 in anterograde axonal trafficking. However, axons still form in both *unc-76* and *unc-116* mutants, with some Stx being present in the axonal membrane, suggesting that the UNC-76/Kinesin-1 transport complex is not the only cargo-motor complex capable of delivering Stx to the axonal plasma membrane (6, 7).

Phosphorylation Regulates FEZ1-Mediated Interactions. In *Drosophila*, phosphorylation of UNC-76 at residue S143 regulates its binding to synaptotagmin and controls loading of kinesin with synaptic vesicles (3). Using liquid chromatography-tandem mass spectrometry (LC-MS/MS), we identified four phospho-serine sites (S58, S134, S301, and S316) from GFP-FEZ1 immunoprecipitated from HEK 293 cell lysates (Fig. S7A). Thus, FEZ1 is also phosphorylated in vivo. Importantly, S58 corresponds to S143 in *Drosophila* UNC-76 and is flanked by highly conserved amino acids (Fig. S7B).

To determine whether FEZ1 phosphorylation affects its binding to Munc18, Stx, and KIF5C, we treated lysates of HEK 293 cells expressing various combinations of the four proteins with alkaline phosphatase (AP) and then tested by immunoprecipitation if any of the interaction was affected by the treatment. Phosphatase treatment virtually abolished interaction of FEZ1 with Munc18 and KIF5C (Fig. 5A and B). In contrast, binding to

Stx was only marginally affected, whereas kinesin binding was abolished regardless of the presence of Stx or Munc18 (Fig. 5 B and C). Intriguingly, Munc18 binding was preserved in the presence of Stx, again demonstrating that Munc18 can bind to the trimeric complexes via its interaction with Stx (Fig. 5D).

To determine which of the phospho-serines is involved in regulating FEZ1 binding to Munc18 and Kinesin-1, we generated a series of FEZ1 point mutations in which one or several of the four identified serines were mutated to alanines. The mutants were then tested in an Y2H assay against KIF5A, KIF5C, and Munc18. Significantly, mutation of the conserved S58 alone specifically abolished its interaction with Munc18 (Table S1). Furthermore, mutation of any other site also disrupted interaction with Kinesin-1. This contrasts with previous observations in *Drosophila* where binding of UNC-76 to Kinesin-1 was not influenced by the phosphorylation status of S143 (3).

Finally, we tested whether S58 is critical for FEZ1/Kinesin-1 transport of Stx in neurons. In these experiments, we took advantage of the fact that human FEZ1 rescues the *unc-76* uncoordinated phenotype (30) and expressed the human protein in *unc-76* mutant strains of *C. elegans*. As expected, wild-type FEZ1 rescued UNC-64 transport defects observed in *unc-76* mutants (Fig. 6). In contrast, expression of FEZ1 S58A did not ameliorate UNC-64 clustering in these mutants. In fact, quantitative image analysis revealed that the clustering phenotype is even more pronounced than observed in *unc-76* mutants. These findings confirm that phosphorylation of FEZ1 at S58 is essential for its function as a cargo adaptor for Kinesin-1-dependent axonal transport of Stx.

Discussion

The trafficking routes involved in biogenesis, maintenance, and turnover of the axonal and presynaptic plasma membrane are largely unclear (1, 31). In contrast to the relatively well-characterized synaptic vesicle precursors, the nature and composition of vesicles carrying proteins such as Stx, presynaptic potassium, and calcium channels is unknown. It is also unclear whether all of these proteins are transported along the axon by a single class of vesicles derived from the Golgi complex as “constitutive” secretory vesicles, or whether several vesicle populations coexist that are differentially regulated. Stx is one of the most abundant neuronal membrane proteins that is concentrated in synapses but that is also widely distributed along the axonal plasma membrane (32, 33). Stx has been detected both in purified synaptic vesicles (34) (albeit is less abundant than in the plasma membrane) and in Piccolo-Bassoon transport vesicles (PTVs) (35), as well as in amyloid-precursor protein (APP)-containing transport vesicles transported by Kinesin-1 (36), but it is unlikely that the bulk of Stx is transported by any of these routes.

Our data show that transport of Stx along axons is mediated in part by KIF5C via its specific adaptor FEZ1. Strong colocalization of Stx, Munc18, and FEZ1 in growth cones from young neurons and data from transgenic worms indicate that transport via FEZ1/Kinesin-1 transport complexes play an important role in bringing Stx and Munc18 to the tips of rapidly developing axons during neuritegenesis. Thus, we identified a second transport complex

for Stx distinct from, but that may act in conjunction with, the previously identified adaptor syntabulin that mediates Stx transport via another member of the Kinesin-1 family (KIF5B) (6, 7). It will be interesting to clarify whether FEZ1 and syntabulin can functionally substitute for each other in the transport of Stx-containing vesicles and whether their cargo spectrum is similar.

Importantly, Munc18 also resides in the same FEZ1/Kinesin-1 transport complex. This observation is significant given previous reports that correct plasma membrane trafficking of Stx strongly depends on the presence of Munc18 (8–13, 22). Noteworthy, Stx is able to bind FEZ1 in the absence of Munc18. Thus, the motor complex is, by itself, unable to correctly distinguish processed Stx (bound by Munc18) from improperly processed (“free”) Stx. Our findings, thus, support the current view that Munc18 serves to protect Stx from spurious interactions during Golgi maturation and provides additional evidence for the involvement of Munc18 in post-Golgi transport of Stx. In the latter role, it is conceivable that the Munc18-FEZ1 interaction serves to signal to the motor that a properly processed cargo has been loaded. The observation that the binding of Munc18 to FEZ1 is also phosphorylation-dependent offers a tantalizing possibility that such events may mediate loading/unloading of Stx trafficking vesicles to KIF5C as has been reported for other Kinesin adaptors (4).

Phosphorylation of UNC-76 by UNC-51 affects the binding of UNC-76 to synaptotagmin and is essential for its axonal transport (3). Flies lacking UNC-51 or expressing a phosphorylation-defective UNC-76 mutant exhibit axonal transport defects resulting from loss of cargo binding to UNC-76. Like its *Drosophila* counterpart, alanine substitution of FEZ1 at the conserved S58 created a phosphorylation-defective mutant that failed to transport UNC-64 along neuronal axons. However, unlike UNC-76, this defect cannot be directly attributed to the loss of cargo binding because Stx remains attached to FEZ1. Instead, lack of phosphorylation at S58 abrogates binding of Munc18 and Kinesin-1. Importantly, we observe that binding of FEZ1 to Kinesin-1 is strictly dependent on phosphorylation at multiple sites (including S58) unlike UNC-76. Conceivably, loss of phosphorylation of FEZ1 detaches the adapter-cargo complexes from the motor, leading to their accumulation within the axon.

Our findings can be integrated into a model where FEZ1 serves to connect Stx-containing transport vesicles to Kinesin-1 to deliver them to the presynapse (Fig. S8). Accordingly, FEZ1 is phosphorylated in the cell body, which activates the protein and promotes binding to both Kinesin-1 and Munc18. Based on our data, Stx has two options for binding: one by directly interacting with FEZ1 in a phosphorylation-independent manner, and the other via binding to Munc18 in an inactive (closed) conformation. Conversely, Munc18 can also bind to FEZ1 via Stx in a phosphorylation-independent manner. Although it is currently not possible to discern between these alternatives, the fact that Munc18 is needed for axonal transport of Stx favors the view that Munc18 binding to FEZ1 constitutes the primary interaction.

After reaching presynaptic sites, activation of phosphatases is expected to dissociate the cargo from the motor protein. Again, it remains to be established whether the Stx cargo vesicles are

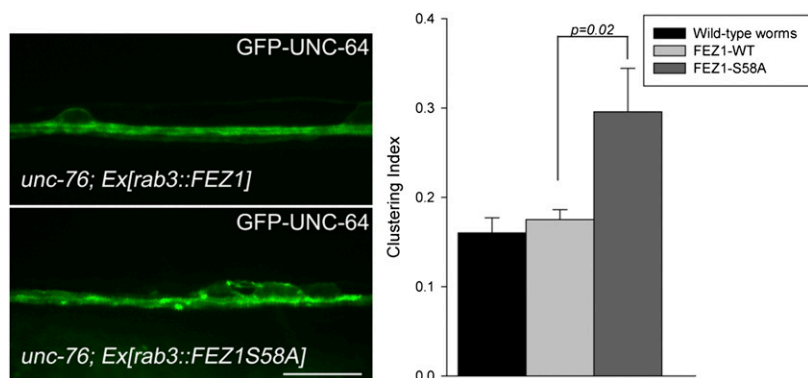


Fig. 6. S58A is essential for phosphorylation-dependent transport of Stx (UNC-64) in axons. Localization of GFP-UNC-64 in VNC of *unc-76(e911)* mutants coexpressing mCherry-FEZ1 (wild-type) or mCherry-FEZ1(S58A). Irregular distribution of GFP-UNC-64 in *unc-76* mutants was rescued by expression of wild-type FEZ1, whereas expression of FEZ1(S58A) aggravated the clustering phenotype of GFP-UNC-64 in these worms. Quantifications of GFP-UNC-64 clustering for both transgenic worms are shown (Right). Eight worms were taken for each analysis. Error bars represent SEM. (Scale bar, 10 μ m.)

also dissociated from FEZ1 or whether the phosphorylation-independent binding of Stx may serve to retain some FEZ1 bound to Stx after reaching the final destination in the synaptic/axonal plasma membrane.

Perturbations of microtubule-based transport are implicated in an increasing number of neurodegenerative diseases (NDs) (37). FEZ1 not only transports Stx but also synaptic vesicles (3) and mitochondria (38). Importantly, FEZ1 also interacts with proteins involved in NDs such as disrupted in schizophrenia 1 (DISC1) (39) and huntingtin (40). We hope that further characterization of FEZ1's role in axonal transport will provide additional insight into how transport disorders contribute to the progression of NDs.

Materials and Methods

Plasmids and Antibodies. All plasmids used in this study were generated by standard cloning. Descriptions of procedures and antibodies used are detailed in *SI Materials and Methods*.

Automated Y2H Screening. Automated Y2H screening was carried out as published previously with minor modifications (41). Details concerning the screen are provided in *SI Materials and Methods*.

Coimmunoprecipitations. One day after transfection, cells were lysed with ice-cold HNE buffer [50 mM Hepes (pH 7.2), 150 mM NaCl, 1% (vol/vol) Triton X-100, 1 mM EDTA] containing Complete EDTA-free protease inhibitor mixture (Roche). Cell lysates were cleared by centrifugation, and the resultant

supernatant was incubated with anti-FLAG, anti-V5, or anti-GFP antibodies for 3 h. Thirty microliters of protein G-Sepharose were subsequently added to the mixture and incubated continued for an additional hour. Immunoprecipitates were washed 4× with HNE buffer. Proteins were eluted with 2× LDS buffer and analyzed by immunoblotting.

C. elegans Strains. Generation of constructs and worm culturing were performed according to standard procedures. Details are provided in *SI Materials and Methods*.

Immunocytochemistry. Primary hippocampal neurons were fixed with 3.6% (wt/vol) paraformaldehyde at 2–3 d in vitro (DIV). Neurons were permeabilized with 0.3% Triton-X100 in PBS (pH 7.3) and blocked with 10% normal goat serum diluted in PBS. Coverslips were incubated with primary antibodies for 1 h. After washing, cells were incubated with Cy2- or Cy3-conjugated goat anti-rabbit and donkey anti-mouse antibodies, respectively (Jackson ImmunoResearch). Images were acquired using a Leica SP2 confocal microscope.

ACKNOWLEDGMENTS. We thank Maria Druminski, Ina Maria Herfort, Kirstin Rau, and Jan Timm for excellent technical assistance. This work received funding from European Union Sixth and Seventh Framework Programme Grants LSHM-CT-2005-019055 ("EUSynapse") and HEALTH-F2-2009-241498 (European Study Programme in Neuroinformatics "EuroSPIN") and from National Genome Research Network (NGFN) Grants NGFNp NeuroNet-TP1/TP3, 01GS08170, and 01GS08171. M.G. was supported by a research fellowship from The Alfred Benzon Foundation.

- Hirokawa N, Noda Y, Tanaka Y, Niwa S (2009) Kinesin superfamily motor proteins and intracellular transport. *Nat Rev Mol Cell Biol* 10:682–696.
- Gindhart JG, et al. (2003) The kinesin-associated protein UNC-76 is required for axonal transport in the *Drosophila* nervous system. *Mol Biol Cell* 14:3356–3365.
- Toda H, et al. (2008) UNC-51/ATG1 kinase regulates axonal transport by mediating motor-cargo assembly. *Genes Dev* 22:3292–3307.
- Horiuchi D, et al. (2007) Control of a kinesin-cargo linkage mechanism by JNK pathway kinases. *Curr Biol* 17:1313–1317.
- Koushika SP (2008) "JIP"ping along the axon: The complex roles of JIPs in axonal transport. *Bioessays* 30:10–14.
- Su Q, Cai Q, Gerwin C, Smith CL, Sheng ZH (2004) Syntabulin is a microtubule-associated protein implicated in syntaxin transport in neurons. *Nat Cell Biol* 6:941–953.
- Cai Q, Pan PY, Sheng ZH (2007) Syntabulin-kinesin-1 family member 5B-mediated axonal transport contributes to activity-dependent presynaptic assembly. *J Neurosci* 27:7284–7296.
- Rowe J, Calegari F, Taverna E, Longhi R, Rosa P (2001) Syntaxin 1A is delivered to the apical and basolateral domains of epithelial cells: The role of munc-18 proteins. *J Cell Sci* 114:3323–3332.
- Han L, et al. (2009) Rescue of Munc18-1 and -2 double knockdown reveals the essential functions of interaction between Munc18 and closed syntaxin in PC12 cells. *Mol Biol Cell* 20:4962–4975.
- Medine CN, Rickman C, Chamberlain LH, Duncan RR (2007) Munc18-1 prevents the formation of ectopic SNARE complexes in living cells. *J Cell Sci* 120:4407–4415.
- Rowe J, et al. (1999) Blockade of membrane transport and disassembly of the Golgi complex by expression of syntaxin 1A in neurosecretion-incompetent cells: Prevention by rbSEC1. *J Cell Sci* 112:1865–1877.
- Rizo J, Rosenmund C (2008) Synaptic vesicle fusion. *Nat Struct Mol Biol* 15:665–674.
- Arunachalam L, et al. (2008) Munc18-1 is critical for plasma membrane localization of syntaxin1 but not of SNAP-25 in PC12 cells. *Mol Biol Cell* 19:722–734.
- McEwen JM, Kaplan JM (2008) UNC-18 promotes both the anterograde trafficking and synaptic function of syntaxin. *Mol Biol Cell* 19:3836–3846.
- Toonen RF, de Vries KJ, Zalm R, Südhof TC, Verhage M (2005) Munc18-1 stabilizes syntaxin 1, but is not essential for syntaxin 1 targeting and SNARE complex formation. *J Neurochem* 93:1393–1400.
- Assmann EM, Alborghetti MR, Camargo ME, Kobarg J (2006) FEZ1 dimerization and interaction with transcription regulatory proteins involves its coiled-coil region. *J Biol Chem* 281:9869–9881.
- Lanza DC, et al. (2009) Human FEZ1 has characteristics of a natively unfolded protein and dimerizes in solution. *Proteins* 74:104–121.
- Blasius TL, Cai D, Jih GT, Toret CP, Verhey KJ (2007) Two binding partners cooperate to activate the molecular motor Kinesin-1. *J Cell Biol* 176:11–17.
- Okada Y, Yamazaki H, Sekine-Aizawa Y, Hirokawa N (1995) The neuron-specific kinesin superfamily protein KIF1A is a unique monomeric motor for anterograde axonal transport of synaptic vesicle precursors. *Cell* 81:769–780.
- Zhao C, et al. (2001) Charcot-Marie-Tooth disease type 2A caused by mutation in a microtubule motor KIF1Bbeta. *Cell* 105:587–597.
- Maturana AD, Fujita T, Kuroda S (2010) Functions of fasciculation and elongation protein zeta-1 (FEZ1) in the brain. *ScientificWorldJournal* 10:1646–1654.
- Cotrufo T, et al. (2011) A signaling mechanism coupling netrin-1/deleted in colorectal cancer chemoattraction to SNARE-mediated exocytosis in axonal growth cones. *J Neurosci* 31:14463–14480.
- Steiner P, et al. (2002) Overexpression of neuronal Sec1 enhances axonal branching in hippocampal neurons. *Neuroscience* 113:893–905.
- Koushika SP, Nonet ML (2000) Sorting and transport in *C. elegans*: A model system with a sequenced genome. *Curr Opin Cell Biol* 12:517–523.
- Su CW, et al. (2006) The short coiled-coil domain-containing protein UNC-69 cooperates with UNC-76 to regulate axonal outgrowth and normal presynaptic organization in *Caenorhabditis elegans*. *J Biol* 5:9.
- Hosono R, et al. (1992) The unc-18 gene encodes a novel protein affecting the kinetics of acetylcholine metabolism in the nematode *Caenorhabditis elegans*. *J Neurochem* 58:1517–1525.
- Saifee O, Wei L, Nonet ML (1998) The *Caenorhabditis elegans* unc-64 locus encodes a syntaxin that interacts genetically with synaptobrevin. *Mol Biol Cell* 9:1235–1252.
- Ogawa H, Harada S, Sassa T, Yamamoto H, Hosono R (1998) Functional properties of the unc-64 gene encoding a *Caenorhabditis elegans* syntaxin. *J Biol Chem* 273:2192–2198.
- Patel N, Thierry-Mieg D, Mancillas JR (1993) Cloning by insertional mutagenesis of a cDNA encoding *Caenorhabditis elegans* kinesin heavy chain. *Proc Natl Acad Sci USA* 90:9181–9185.
- Bloom L, Horvitz HR (1997) The *Caenorhabditis elegans* gene unc-76 and its human homologs define a new gene family involved in axonal outgrowth and fasciculation. *Proc Natl Acad Sci USA* 94:3414–3419.
- Goldstein AY, Wang X, Schwarz TL (2008) Axonal transport and the delivery of presynaptic components. *Curr Opin Neurobiol* 18:495–503.
- Garcia EP, McPherson PS, Chilcote TJ, Takei K, De Camilli P (1995) rbSec1A and B colocalize with syntaxin 1 and SNAP-25 throughout the axon, but are not in a stable complex with syntaxin. *J Cell Biol* 129:105–120.
- Koh S, et al. (1993) Immunoelectron microscopic localization of the HPC-1 antigen in rat cerebellum. *J Neurocytol* 22:995–1005.
- Walch-Solimena C, et al. (1995) The t-SNAREs syntaxin 1 and SNAP-25 are present on organelles that participate in synaptic vesicle recycling. *J Cell Biol* 128:637–645.
- Zhai RG, et al. (2001) Assembling the presynaptic active zone: A characterization of an active one precursor vesicle. *Neuron* 29:131–143.
- Szodorai A, et al. (2009) APP anterograde transport requires Rab3A GTPase activity for assembly of the transport vesicle. *J Neurosci* 29:14534–14544.
- De Vos KJ, Grierson AJ, Ackerley S, Miller CC (2008) Role of axonal transport in neurodegenerative diseases. *Annu Rev Neurosci* 31:151–173.
- Fujita T, et al. (2007) Axonal guidance protein FEZ1 associates with tubulin and kinesin motor protein to transport mitochondria in neurites of NGF-stimulated PC12 cells. *Biochem Biophys Res Commun* 361:605–610.
- Miyoshi K, et al. (2003) Disrupted-In-Schizophrenia 1, a candidate gene for schizophrenia, participates in neurite outgrowth. *Mol Psychiatry* 8:685–694.
- Goehler H, et al. (2004) A protein interaction network links GIT1, an enhancer of huntingtin aggregation, to Huntington's disease. *Mol Cell* 15:853–865.
- Stelzl U, et al. (2005) A human protein-protein interaction network: A resource for annotating the proteome. *Cell* 122:957–968.